Applied Physics Letters

A dynamic operation of a PIN photodiode

Cite as: Appl. Phys. Lett. **106**, 031115 (2015); https://doi.org/10.1063/1.4906488
Submitted: 23 May 2014 • Accepted: 12 January 2015 • Published Online: 22 January 2015

S. Okhonin, M. Gureev, D. Sallin, et al.

A dynamic operation of a PIN photodiode

S. Okhonin,[1,a)] M. Gureev,[1] D. Sallin,[2] J. Appel,[3] A. Koukab,[2] A. Kvasov,[4] M. Pastre,[2] E. S. Polzik,[3] A. K. Tagantsev,[4,5] F. Uddegard,[1] and M. Kayal[2]
[1]*ActLight SA, EPFL Innovation Park, Building I, 1015 Lausanne, Switzerland*
[2]*Electronics laboratory, École Polytechnique Fédérale de Lausanne (EPFL), 1015 Lausanne, Switzerland*
[3]*The Niels Bohr Institute, University of Copenhagen, Copenhagen DK-2100, Denmark*
[4]*Ceramics laboratory, École Polytechnique Fédérale de Lausanne (EPFL), 1015 Lausanne, Switzerland*
[5]*Ioffe Physical Technical Institute, 194021 St. Petersburg, Russia*

(Received 23 May 2014; accepted 12 January 2015; published online 22 January 2015)

Traditionally, photodiodes operate at static reverse bias, and incident light intensity is obtained from the relatively week photocurrent. In this paper, we introduce a different concept of photodiode function: the photodiode is used in a dynamic regime where it is switched from the reverse to forward state. Thus, the light intensity is defined not by the measured photocurrent but by the delay time of appearance of the strong forward current with the amplitude independent of the light intensity. Our experimental results as well as finite element modeling show that the dynamic mode of photodiode operation can potentially provide an improvement of the device performance. © *2015 AIP Publishing LLC*. [http://dx.doi.org/10.1063/1.4906488]

Semiconductor diodes are the most common type of photodetectors and are widely used in the electronics industry in a variety of areas from ambient light sensors to wide bandwidth optical telecommunications systems. The technology of diodes functioning as photodetectors (photodiodes) was developed long ago, in the 1950s. Apart from the introduction of the PIN photodiode at the end of the same decade, conceptually, nothing changed since that time. A PIN photodiode contains two strongly p- and n-doped regions separated by a weakly doped (or undoped) region (schematically shown in Fig. 1(a)). The light-induced carrier generation in the PIN structure was initially investigated by Gartner[1] in 1959, paving the way to the widespread use in industrial applications. Since that time, all PIN photodiodes operate the same way: A constant reverse bias is applied and the incident light intensity is obtained from the measured photocurrent, which we will call the *static regime*. So far, to improve the characteristics of PIN diodes, the research was mainly focused on the geometry optimization and use of new materials, but the fundamental limitations related to the small output current cannot be resolved within this approach.

A schematic dark current-voltage (I-V) curve of a PIN diode is shown in Fig. 1(b). In the standard static regime, the diode is kept at a fixed reverse bias (point A in Fig. 1(b)), where the dark current is very small. Under illumination, the device current increases proportionally to the rate of absorbed photons. However, this photocurrent is rather small for the weak light, and an external amplifier is generally required. In the real applications, an amplifier is often the main source of noise at the week light conditions.

A high output signal can be achieved by using photodetectors with an internal gain. The most well known detector of this type is an avalanche photodiode, where the impact ionization mechanism is used for internal amplification.[2–4] Such detectors always operate at high voltages that limit their use to only specific applications.

In this paper, we introduce the Dynamic PhotoDiode (DPD) concept: an operating mode of a PIN diode where the applied voltage is switched as is shown in Fig. 1(c) from reverse to forward (from point A to point B in Fig. 1(b)). Applied forward bias induces a large forward current after a time delay (Fig. 1(d)). The forward current magnitude is controlled only by the applied forward voltage value (see point B on Fig. 1(b)), and it does not depend on the light intensity. In contrast, the delay time is a function of the absorbed light power.

Measuring the delay time of photocurrent instead of its magnitude provides a different way of light sensing. The DPD brings several important features. (i) It has high output signal, which is normally several orders of magnitude higher than that of a standard PIN photodiode. (ii) At the same time, the DPD does not use any high electrical field mechanisms such as impact ionization. (iii) Since the delay time is measured, the output signal can be digitalized without any analog-to-digital converters. Here, we should say that, in principle, any PIN photodiode could operate in the proposed dynamic mode, although a device optimization is required to obtain desired characteristics.

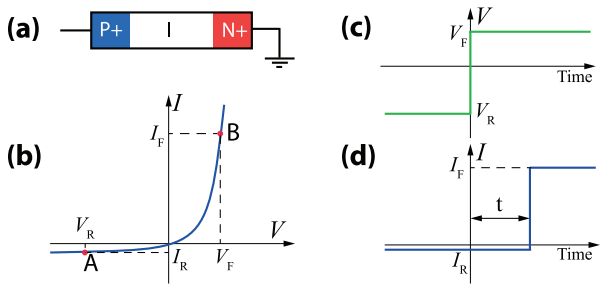

FIG. 1. PIN diode in static and dynamic modes. (a) A schematic PIN diode structure. (b) PIN diode dark I-V curve. (c) Applied voltage and (d) current time dependence for DPD. Triggering (delay) time *t* depends on light intensity.

[a)]Author to whom correspondence should be addressed. Electronic mail: okhonin@act-light.com.

When a PIN photodiode is switched from reverse to forward bias (dynamic operational mode), the forward current appears after some delay. We performed modeling of the dynamic mode of the PIN structure shown on Fig. 2(a) and demonstrated that even a simple device without any optimization has a delay time of order of 100ps (Fig. 2(b)). A short light pulse considerably reduces switching time (triggering time) of the device. This result shows that even this simple PIN diode operated in the dynamic mode may be potentially used in high frequency (more than 10GHz) applications such as high-speed optical data transfer.[2–8]

A device optimization increasing the time delay broadens the domain of possible applications making the DPD suitable, for instance, for low-power portable applications. We propose to use the Complimentary Metal-Oxide-Semiconductor (CMOS) gates placed around P+ regions for optimization. Even though the gates and the P+ contact can be powered independently, we mainly use structures where the gates and the P+ contact are connected, keeping a two-terminal diode configuration. We performed finite element modeling for a large number of devices, and it was found that modifications of the PIN structure changes the delay time to the nanosecond–millisecond range. Figure 3(a) shows the optimized PIN structure for which the delay time in the microsecond range is obtained. Figure 3(b) shows that the triggering time of the optimized device without light (self-triggering time) is in the order of 0.5 μs, which is much longer than for a non-optimized PIN structure. A light pulse considerably decreases this triggering time (Fig. 3(b)).

Based on the modeling results, we designed series of optimized PIN structure prototypes searching for the best characteristics. Devices were fabricated using 180 nm CMOS technology. For the prototype shown in Fig. 4(a) corresponding to the simulated structure in Fig. 3(a), we could achieve a considerable change of the triggering time. Figure 4(b) illustrates the behavior of the device in the dynamic regime described above: the PIN is switched from the reverse to the forward state with the delay time dependent on the continuous light intensity. Remarkably, the switching from the low current to the high-current state occurs very abruptly, which is favorable for the precise measurements of the delay time.

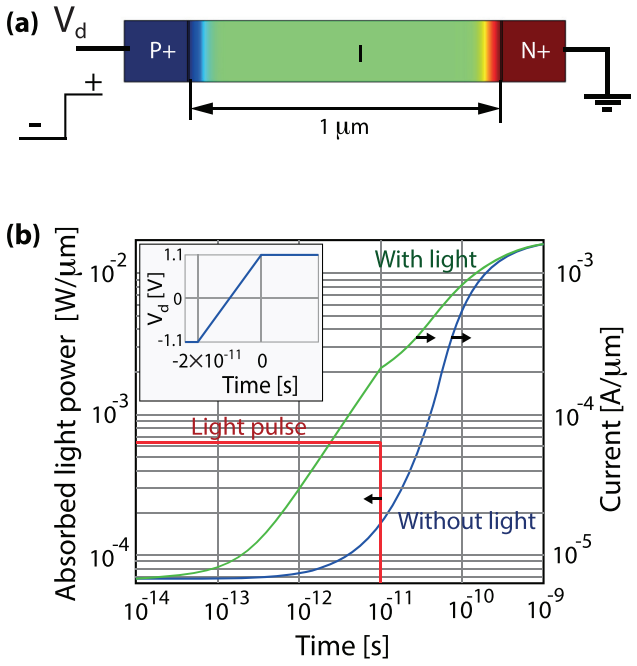

FIG. 2. Modeling of simple PIN diode. (a) Cross-section of modeled PIN diode. (b) I-t dependence of the simplified PIN. Inset shows applied voltage. The modeling results were obtained by means of phase-field simulation using a drift-diffusion model. In the model, a uniform electron-hole generation rate is used. We calculated the absorbed light power assuming a light wavelength of 845 nm.

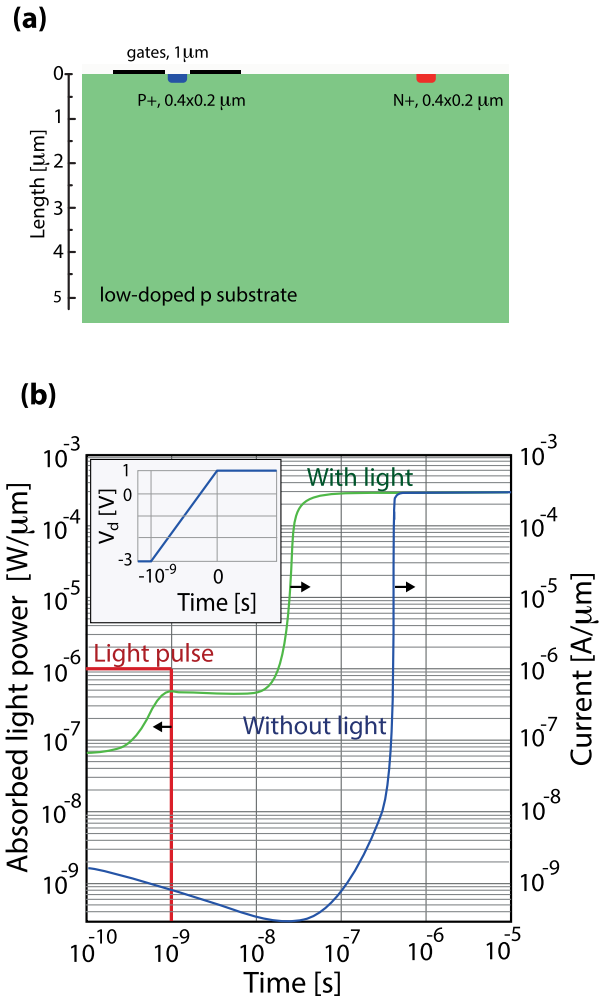

FIG. 3. Modeling of optimized PIN structure. (a) Cross-section of modeled PIN structure. (b) I-t dependence for the optimized device. Inset shows applied voltage. Values of light power and current are given per 1 μm width of the device.

We measured photocurrent of the same device used as a standard photodiode: When N+ is grounded, gate is disconnected and -3 V is applied to P+. The photocurrent of 18 nA was achieved in the standard photodiode mode with the maximum light intensity used in this experiment. At the same time, the DPD output current of 0.8 mA is more than four orders higher compared to the photocurrent of 18 nA. The photocurrent was also used to calibrate light power absorbed in the device as $P = hcI/(e\lambda)$, where I is the photocurrent, h is the Planck constant, c is the speed of light, $\lambda = 635$ nm is the wavelength, and e is the elementary charge.

Typically, the dependence of the reciprocal triggering time on the absorbed light power is close to linear, as it is

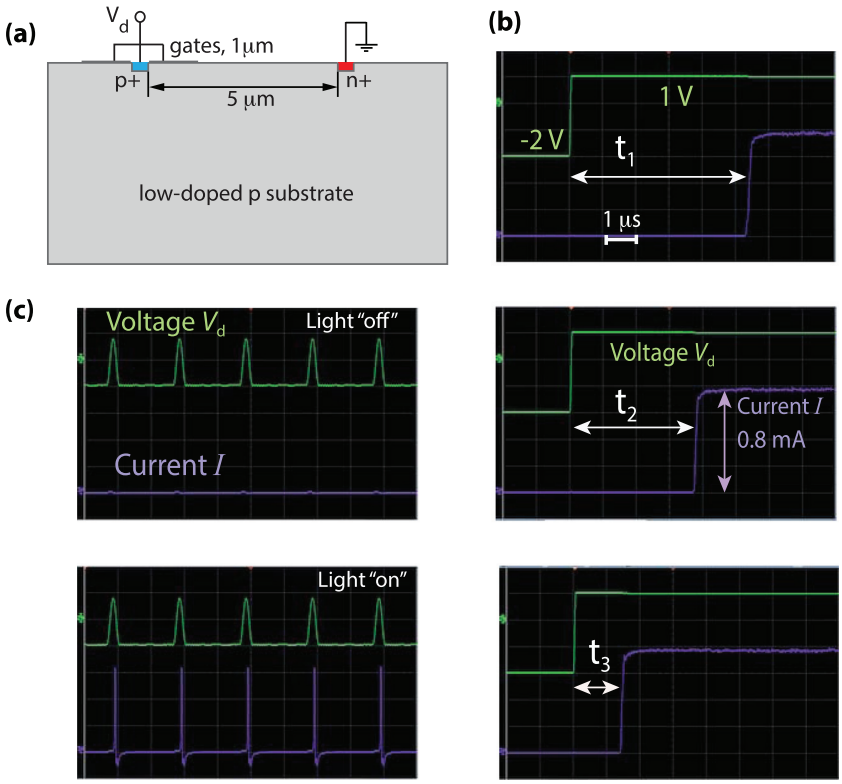

FIG. 4. Prototype of optimized PIN structure and measured output current. (a) Cross-section of the fabricated device. (b) Scope screen shots of applied voltage V_d and output current I at different light intensities. Triggering time t decreases with light intensity increasing. Triggering time $t_1 = 5.5\,\mu s$—no light, $t_2 = 3.8\,\mu s$—absorbed power 6 nW, $t_3 = 1.5\,\mu s$—absorbed power 35 nW. (c) Experiment with pulsed voltage, V_d: 100 ns pulses (forward bias) with 1 us period applied to the DPD. When light is off, the delay time of the output current is more than the pulse width (100 ns); therefore, the output current does not appear. Alternatively, in the presence of light, the triggering time of I is shorter than pulse width and the device produces pulsed output current.

shown on Fig. 5. The same dependence can be obtained for a standard photodiode after light to time or light to frequency conversion, as it is done to increase the dynamic range.[9] Therefore, we conclude that DPD may potentially provide a high dynamic range.

The DPD can be also used as a photodetector operating in the digital regime. When voltage pulses are applied to the DPD (Figure 4(c)), the output current pulses will be seen only if the forward voltage pulse width is longer than the device triggering time. Due to a strong dependence of the device triggering time on the incident light intensity, the threshold light intensity that induces an output current can be selected by changing the forward voltage pulse width.

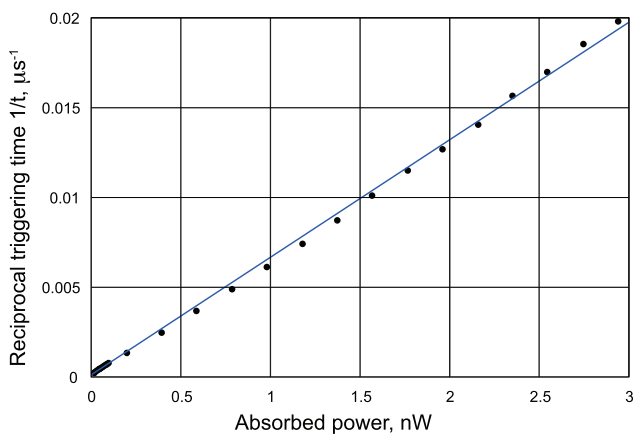

FIG. 5. Reciprocal triggering time as a function of the absorbed light power. The measurements were done with 635 nm continuous wave light source. The device length was 180 μm, device width 10 μm, gate length 1 μm. The absorbed power was extracted from the measurement of reverse biased current performed on the same device.

The physics behind the behavior of PIN photodiode in the dynamic mode can be elucidated as follows. When a reverse bias is applied, the excess carriers are removed from the low-doped region. After switching to the forward bias, the charge in the depletion regions adjacent to N+ and P+ creates potential barriers (shown in Fig. 6(b)), which strongly suppress forward current. It should be noted that the existence of these barriers was pointed out in Ref. 10, where the p-n junction behavior at liquid helium temperature was discussed. Eventually, under the forward bias, the hole and electron currents from P+ and N+ regions, respectively, reduce these potential barriers and forward current flows. The abrupt current increase measured (Fig. 4(b)) and simulated (Fig. 3(b)) is explained by an internal positive feedback mechanism: the holes injected from the P+ contact reduce the potential barrier near the N+ contact and increase the electron injection, which in turn reduces the potential barrier near the P+ contact and increases the hole current. If the incident light is present, the barriers still exist after voltage switching, but the induced photo carriers accelerate the barrier lowering and reduce the time delay.

In the case of a simple PIN diode, the potential barriers are rather small (Figs. 6(a) and 6(b)) and the triggering time without light is in the order of 100ps (Fig. 2(b)). In view of the physical mechanism described above, the device optimization consists of changing of potential barrier parameters as was done for the optimized PIN geometry by introducing the gates with applied voltage (Figs. 6(c) and 6(d)).

We found that the following qualitative model explains well DPD triggering behavior: the device triggers when certain critical number of electrons N_{crit} is accumulated in the barrier region. Thus, the triggering time can be estimated as $T = N_{crit}/(G + G_{dark})$, where G is the light-induced

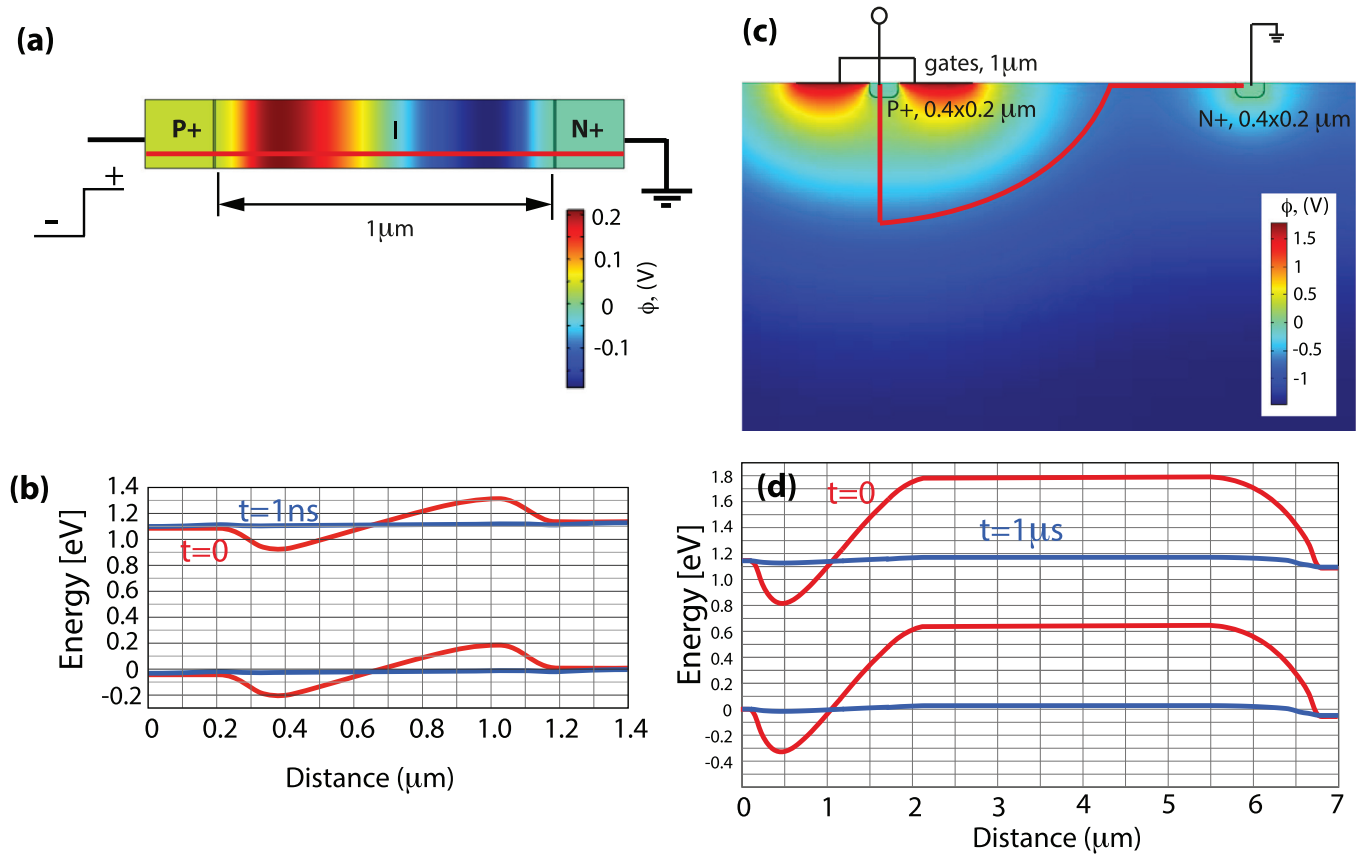

FIG. 6. Band diagrams. (a) Simple PIN diode cross-section with simulated potential just after switching to the forward voltage. (b) Band diagram along the cutline (red line in Fig. 6(a)) just after switching to the forward voltage (at time t = 0) and at the moment when forward current approaches its stationary value (t = 1 ns), see Fig. 2(b). (c) Cross section and simulated potential just after switching to the forward voltage for optimized device. Red line shows the cutline for band diagram (Fig. 6(d)) passing through minimal potential barriers. V_d is applied voltage (see Fig. 3(b)). (d) Band diagram for optimized structure along the cutline just after switching to the forward voltage (t = 0) and at the moment when forward current has its stationary value (t = 1 μs, see Fig. 3(b)).

generation rate (which is proportional to the absorbed light power at a fixed wavelength) and G_{dark} is the dark generation rate (analog of a dark current). Thus, $1/T = (G + G_{dark})/N_{crit}$, i.e., dependence of the reciprocal triggering time on the absorbed incident light power should be linear, as it can be seen on the experimental dependence in Fig. 5. Of course, the simple model described above does not take into account all phenomena that influence the device behavior. For example, it assumes that all electrons generated in the device immediately reach the gate. In reality, the situation is more complex, and experimental dependence may deviate from the linear one, as it is shown in Fig. 5.

By scaling down[11–13] the CMOS technology, it is possible to decrease the internal capacitance of the device, i.e., the charge N_{crit} needed to trigger the DPD. Our estimates show that with the gate length below 10 nm, single photon sensing may be achieved. This way, we propose a low voltage single photon detector. It should be noted that all existing single photon detectors use a high-voltage avalanche mechanism to achieve high internal gain,[14–16] which makes it challenging to use these devices in low power applications.

The present work introduces the dynamic photodiode. The concept is very general and can be applied to multiple types of PIN photodiodes. Potentially, any PIN photodiode can be used in the dynamic mode, although device optimization is required to achieve characteristics required for specific applications. An outstanding feature of the DPD is a high output signal, which eliminates the need for a transimpedance amplifier or comparator, enabling direct interfacing of the DPD output to digital CMOS circuits.

Research was partially supported by the Swiss National Funding (No. 200021_140447) and the government of the Russian Federation (Grant No. 2012-220-03-434, Contract No. 14.B25.31.0025).

[1]W. W. Gartner, Phys. Rev. **116**, 84 (1959).
[2]Y. Kang, H.-D. Liu, M. Morse, M. J. Paniccia, M. Zadka, S. Litski, G. Sarid, A. Pauchard, Y.-H. Kuo, H.-W. Chen, W. S. Zaoui, J. E. Bowers, A. Beling, D. C. McIntosh, X. Zheng, and J. C. Campbell, Nat. Photonics **3**, 59 (2009).
[3]S. Assefa, F. Xia, and Y. A. Vlasov, Nature **464**, 80 (2010).
[4]S. Zhu, K.-W. Ang, S. C. Rustagi, J. Wang, Y. Z. Xiong, G. Q. Lo, and D. L. Kwong, IEEE Electron Dev. Lett. **30**(9), 934 (2009).
[5]J. Michel, J. Liu, and L. C. Kimerling, Nat. Photonics **4**(8), 527 (2010).
[6]L. Vivien, A. Polzer, D. Marris-Morini, J. Osmond, J. M. Hartmann, P. Crozat, E. Cassan, C. Kopp, H. Zimmerman, and J.-M. Fedeli, Opt. Express **20**(2), 1096 (2012).
[7]L. Virot, L. Vivien, J. M. Hartmann, J.-M. Fedeli, D. Marris-Morini, E. Cassan, C. Baudot, and F. Boeuf, Proc. SPIE **8767**, 87670A (2013).
[8]F. Xia, T. Mueller, Y.-M. Lin, A. Valdes-Garcia, and P. Avouris, Nat. Nanotechnol. **4**, 839 (2009).
[9]X. Wang, W. Wong, and R. Hornsey, IEEE Trans. Electron Devices **53**, 2988 (2006).

[10]E. Simoen, B. Dierickx, I. Deferm, and C. Claeys, J. Appl. Phys. **70**, 1016 (1991).
[11]V. A. Sverdlov, T. J. Walls, and K. K. Likharev, IEEE Trans. Electron Devices **50**, 1926 (2003).
[12]S. Deleonibus, ECS Trans. **44**(1), 41 (2012).
[13]H. Iwai, Microelectron. Eng. **86**, 1520 (2009).
[14]S. Cova, M. Ghioni, A. Lacaita, C. Samori, and F. Zappa, Appl. Opt. **35**, 1956 (1996).
[15]C. Niclass, A. Rochas, P.-A. Besse, and E. Charbon, IEEE J. Solid-State Circuits **40**, 1847 (2005).
[16]Y.-S. Kim, Y.-C. Jeong, S. Sauge, V. Makarov, and Y.-H. Kim, Rev. Sci. Instrum. **82**, 093110 (2011).